

OBSERVATION OF RYDBERG TRANSITIONS IN RESONANCE FLUORESCENCE OF ULTRACOLD LITHIUM-7 ATOMS

V. A. Sautenkov,^{1,2*} S. A. Saakyan,¹ E. V. Vilshanskaya,^{1,3} B. B. Zelener,^{1,4}
and B. V. Zelener¹

¹*Joint Institute for High Temperatures, Russian Academy of Sciences
Izhorskaya Street 13, Bd. 2, Moscow 125412, Russia*

²*Lebedev Physical Institute, Russian Academy of Sciences
Leninskii Prospect 53, Moscow 119991, Russia*

³*National Research University – Moscow Power Engineering Institute
Krasnokazarmennaya 17, Moscow 111250, Russia*

⁴*National Research Nuclear University – Moscow Engineering Physics Institute
Kashirskoye Chaussee 31, Moscow 115409, Russia*

*Corresponding author e-mail: vsautenkov@gmail.com

Abstract

We describe our experimental technique for preparation and study of ultracold gas of Rydberg atoms. A magneto-optical trap for ${}^7\text{Li}$ atoms is assembled. Using an ultraviolet laser, we perform a cw two-step excitation of atoms in the ground state to highly-excited states. For identification of highly-excited Rydberg states ($n = 41$ and 110), we record the resonance fluorescence of ultra-cold atoms in the trap.

Keywords: laser cooling, magneto-optical trap, high-resolution spectroscopy, Rydberg atoms.

1. Introduction

Our goal is to prepare and study ultra-cold Rydberg gases and strongly coupled plasmas [1, 2]. A challenge is to create self-organized crystal structures from Rydberg atoms [3–6]. The results of such investigations may be useful for fundamental physics and different applications. Atoms can be effectively transferred to definite Rydberg states by two-photon or multiphoton excitation [1, 7, 8]. The important part of a research work with Rydberg atoms is diagnostic of highly-excited states. In addition to the traditional approach, such as induced ionization of Rydberg atoms by applying an electric field [1], recently new techniques, such as electromagnetically induced transparency [9] and four-wave mixing [10], have been used for diagnostics of the Rydberg transitions. As a first step in our research project, we have realized the cw two-step excitation of ultra-cold lithium atoms from the ground state to the highly-excited Rydberg states.

In this paper, we describe our experimental setup and direct observation of the Rydberg transitions in the resonance fluorescence of ${}^7\text{Li}$ atoms in a magneto-optical trap (MOT). A generic description of the MOT for lithium atoms is presented in [11]. Our setup is similar to an experimental apparatus developed for investigation of the Fermi gas of ${}^6\text{Li}$ atoms [12].

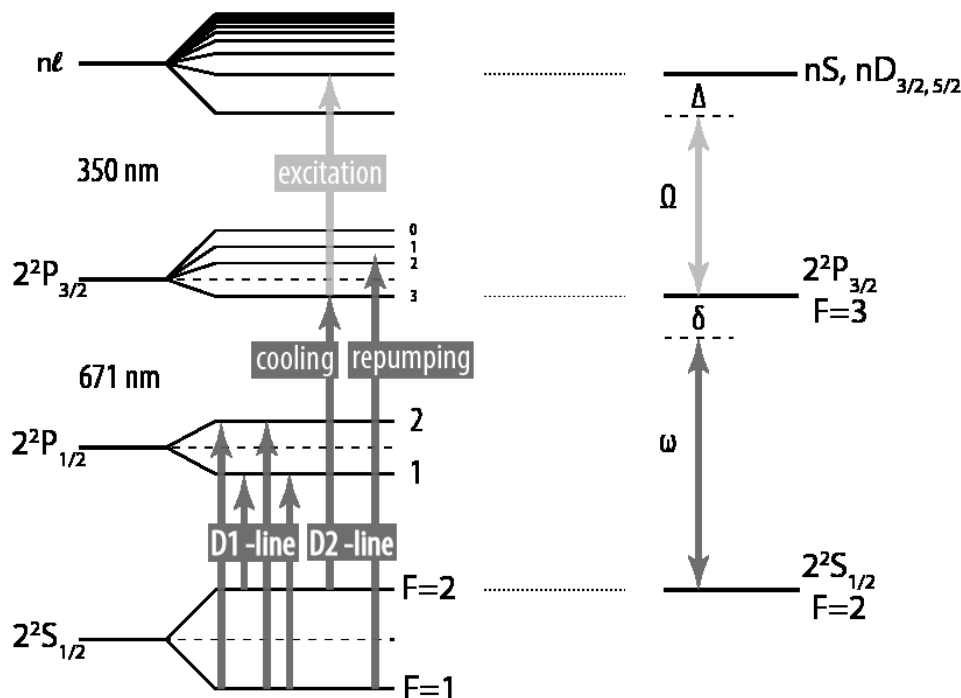


Fig. 1. Diagram of energy levels in ${}^7\text{Li}$ atom.

The atomic transitions in ${}^7\text{Li}$ atom used in our experiments are shown in Fig. 1. Optical transitions in D₂ line are used for optical cooling and trapping of lithium atoms. Optical transitions in D₁ line are used for absorption measurements of an atomic cloud in the MOT using a weak probe laser. In Fig. 1, the light gray arrow indicates an ultraviolet transition (350 nm) from the excited state $2P_{3/2}$ to a highly excited state $n\ell$.

2. Experimental Apparatus

In our laboratory, an experimental setup for trapping and ultraviolet excitation of ${}^7\text{Li}$ atoms is assembled. The apparatus is briefly described in [13, 14]. The setup consists of vacuum and optical systems. The vacuum system includes an oven (the source of a thermal atomic beam), a Zeeman slower, and a main vacuum chamber (residual air pressure $< 10^{-9}$ Torr), where ${}^7\text{Li}$ atoms are trapped.

In the optical part of the setup, we use two amplified external-cavity diode lasers (ECDL) for the cooling and trapping of ${}^7\text{Li}$ atoms. One of them is the cooling laser, which is slightly detuned from the cycling transition $2S_{1/2}$ ($F = 2$) – $2P_{3/2}$ ($F' = 3$). The laser is locked to the thermally stabilized reference cavity with tunable transmission resonances. The other laser is a re-pump laser locked close to the Doppler-free saturation resonance in a hot lithium atomic vapor ($T \sim 700$ K). The laser frequency is detuned by 20 MHz from the transition $2S_{1/2}$ ($F = 1$) – $2P_{3/2}$ ($F' = 2$). The re-pump laser needs to return atoms from sublevel $F = 1$ to sublevel $F = 2$ in the ground state. The optical beams from these two lasers are recombined by polarized beam splitters (PBS) and wave plates to several beams with circular polarization. An optical beam with power near 100 mW is used in the Zeeman slower. Other optical beams with a total power of 150 mW are sent to the vacuum chamber to cool and trap ${}^7\text{Li}$ atoms. The diameters of the optical beams in the vacuum chamber are equal to 2.4 cm. For characterization

of the cloud of ultra-cold atoms, we use a weak probe ECDL. Also our setup includes an ultraviolet laser system ($\lambda \approx 350$ nm) to create Rydberg atoms and a near infrared ECDL ($\lambda \approx 797$ nm) to probe fluorescence of Rydberg atoms.

3. The MOT Parameters

Using the CCD camera, we measured the intensity profile of fluorescence from the atomic cloud in the MOT. The results of the measurements are presented in Fig. 2, which correspond to a magnetic field gradient of 21 G/cm. The profiles of the atomic cloud are very close to the Gaussian distribution with diameters (FWHM) $d_x = 0.24$ cm and $d_y = 0.16$ cm.

Complementary, high-resolution spectroscopy of ^7Li atoms in the MOT is performed by the probe laser. The diameter of the probe beam is much less than the size of the cloud. The intensity of the probe beam is reduced to ensure the regime of linear absorption. The results are presented in Fig. 3.

As one can see, the hyperfine splitting of D_1 line is resolved, whereas the hyperfine splitting of D_2 line is not resolved. In general, both spectra can be used to estimate the number density of atoms in the MOT.

In order to improve the accuracy, we estimated the population of the ground-state sublevels, using

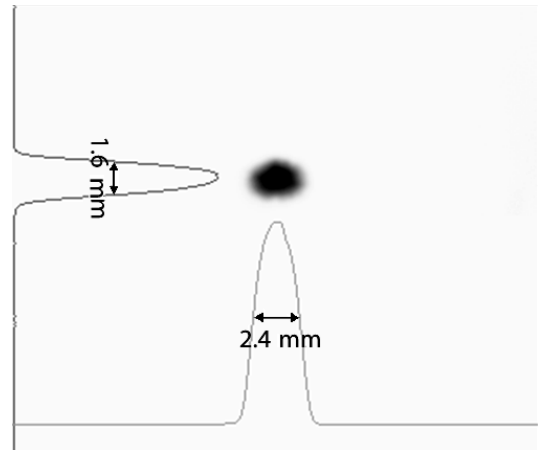


Fig. 2. Atomic cloud in magneto-optical trap.

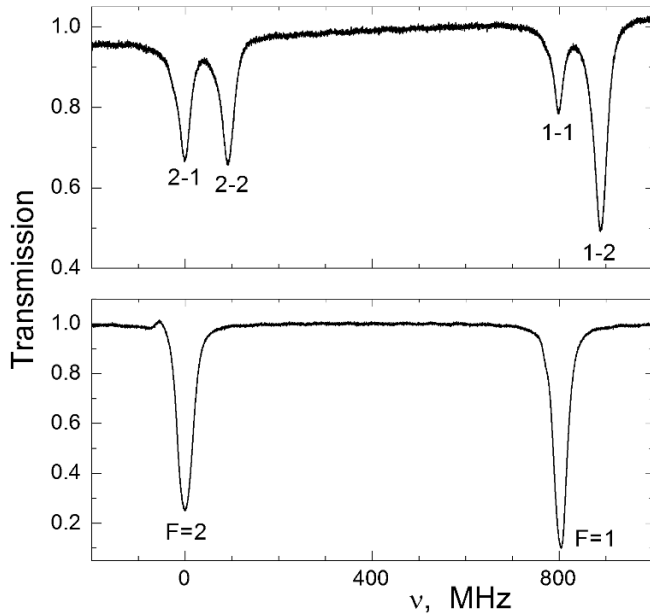


Fig. 3. Transmission of the atomic cloud on D_1 (up) and D_2 (down) lines.

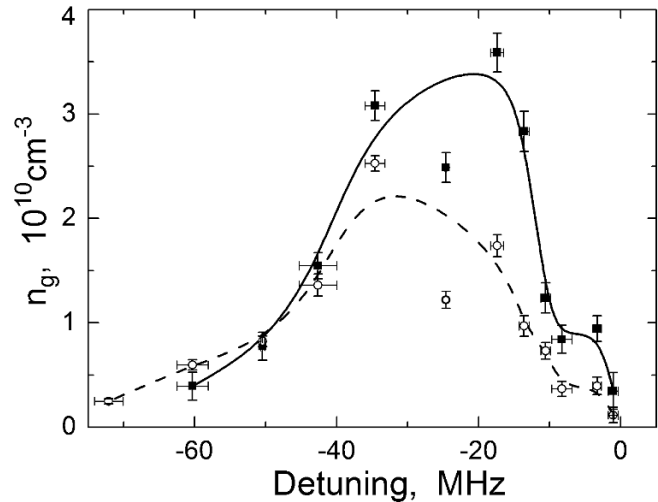


Fig. 4. Concentration of trapped atoms on sublevels $F = 2$ and $F = 1$ of the ground state $2S_{1/2}$. The experimental data for concentrations n_{g1} on sublevel $F = 1$ (■) and n_{g2} on sublevel $F = 2$ (○). The curves serve as guides for the eye.

the transmission spectra of D_1 line. In this case, the absorption is relatively small, and excited state $2P_{1/2}$ is unpopulated. The concentration of the trapped atoms on the sublevel F_g of the ground state $2S_{1/2}$ can be calculated from measured transmittance T , in view of the Beer law,

$$T = \exp[-\sigma(F_g, F_e)nd_x]. \quad (1)$$

We adopted the expression for the absorption cross section for the hyperfine components of D_1 line from [15]; it reads

$$\sigma(F_g, F_e) = \frac{\lambda^2}{4\pi} \frac{A}{\Gamma} \frac{g(F_g, F_e)(2J_e + 1)}{(2J_g + 1)}. \quad (2)$$

Here, A is the Einstein coefficient and Γ is the spectral width of the atomic transition; in our case, $A = \Gamma = 2\pi\gamma$. A natural spectral width of the transition γ is 6 MHz. The factor $g(F_g, F_e)$ can be expressed using 6J symbols [16]. The calculated concentrations of the ground-state atoms versus detuning of the cooling laser are shown in Fig. 4.

Note that the populations of the ground-state $2S_{1/2}$ sublevels are quite close in magnitude. This can be explained by the fact that the upper state $2P_{3/2}$ sublevels are not resolved (hf-splitting is of the same order as the natural width γ). Therefore, it is impossible to select the circling transition for the effective optical cooling. Atoms are continuously transferred from $F = 2$ to $F = 1$ and back. In the maximum (detuning range from 3γ to 6γ), the estimated population of the excited state $2P_{3/2}$ is of the order 10^{-2} of the total population of the ground state. Therefore, the maximum total density of the trapped atoms n is near $5 \cdot 10^{10} \text{ cm}^{-3}$. Under these experimental conditions, the estimated total number N of the trapped atoms is $4 \cdot 10^8$. The estimated temperature of the trapped atoms is of the order of $5 \cdot 10^{-4} \text{ K}$. The concentration n and total number N of atoms can be enhanced by increasing the magnetic field gradient. The linear dependence of n and N on the magnetic field gradient in the range 20 – 35 Gauss/cm has been observed earlier [14].

With the help of the CCD camera, we studied the loading and decay processes in the MOT. In order to prepare the measurements, the de-accelerating optical beam in the Zeeman slower was switched off. Then the de-accelerating beam was switched on, and the loading curve was recorded. When the fluorescence signal reached its maximum value, the de-accelerating beam was switched off again, and the decay curve was recorded. The loading and decay curves recorded at the optimum cooling laser detuning ($\approx 20 \text{ MHz}$) and field gradient 21 Gauss/cm are shown in Fig. 5. The loading (τ_{load}) and decay (τ_{dec}) times are 23 s and 26 s, respectively.

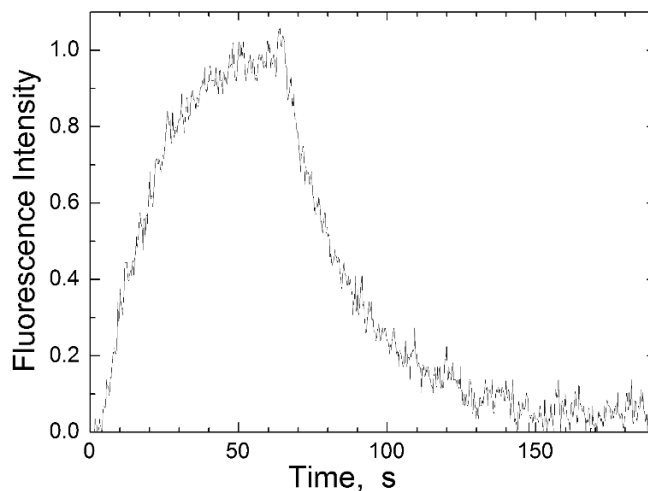


Fig. 5. Loading and decay curves.

4. Two-Step Excitation of Rydberg Atoms

A preliminary observation of the two-step excitation of Rydberg atoms in the resonance fluorescence of lithium atoms was reported in [17]. In the present work, the spectral resolution is improved. For

excitation of Rydberg atoms, we use ultraviolet laser system (Newport Spectra Physics). This cw laser system emits coherent light at a wavelength of 350 nm with an output power up to 100 mW. The laser linewidth is less than 10 MHz and is defined by a short-term stability.

The ultraviolet laser beam (diameter ≈ 1 cm) is sent onto the atomic cloud, and the laser frequency can be continuously tuned. When the ultraviolet laser frequency passes through the Rydberg transition, we observe the reduction of the resonance fluorescence of the trapped atoms. It has gone down to its partial or complete vanishing depending on the ultraviolet laser-beam power and the quantum number of a highly-excited Rydberg state. The reduction of the fluorescence is due to the two-step excitation of lithium atoms.

The frequency of the ultraviolet laser is controlled by a high precision wavemeter WSU (High Finesse-Angstrom). In our experiment, the wavemeter was calibrated using a stabilized ECDL, whose frequency was locked to the Doppler-free absorption resonance in rubidium-85 atomic vapor. According to the selection rules, transitions from the P states are possible only to the nS and nD states. In the experiment, we have measured frequencies ν_{nl} of Rydberg transitions $2P_{3/2}-nl$. To identify Rydberg states, we calculated the quantum numbers nl , taking into account the quantum defect Δn and using the expression [8, 17, 18]

$$n^* = \sqrt{\frac{\text{Ry}}{\nu_i - \nu_{\text{SP}} - \nu_{nl}}}. \quad (3)$$

Here, n^* is the quantum number with quantum defect Δn , Ry is the Rydberg constant for ${}^7\text{Li}$ atoms, ν_i is the ionization threshold frequency for ${}^7\text{Li}$ atoms, and ν_{SP} is a frequency interval between the centers of gravity of the $2S_{1/2}$ and $2P_{3/2}$ states.

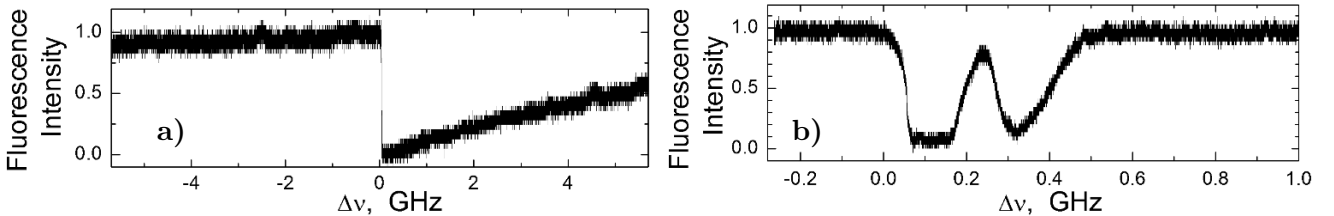


Fig. 6. Resonance fluorescence of the trapped atoms near the transition $2P_{3/2} - 41D$ recorded with fast (a) and slow (b) scan of the laser frequency.

In the first measurements, a high scanning rate of the laser frequency (~ 1 GHz/s) was used. The signal of the resonance fluorescence around Rydberg transition $2P_{3/2} - 41D$ is shown in Fig. 6 a. The dip in the fluorescence signal is attributed to the transition of the ground-state lithium atoms to the Rydberg state by a two-step excitation process.

Here, due to the high scanning rate, the spectral resolution is quite low. One can see the step reduction of the resonance fluorescence due to the resonance two-step excitation, and then the smooth growing of the resonance fluorescence due to the MOT loading. Our preliminary observations of this transition and other Rydberg transitions obtained with the same low spectral resolution are presented in [18]. Recently we have improved the long-term frequency stability of the laser system. The improvements allow us to reduce the scanning rate to a value less than 0.1 GHz/s and increase the spectral resolution. The signal of the resonance fluorescence obtained with better spectral resolution is shown in Fig. 6 b. Here, two components $D_{3/2}$ and $D_{5/2}$ of the $41D$ -state are presented. The average measured frequency of the transition $2P_{3/2} - 41D$ is 854944.8(3) GHz. In the stationary regime, when the signal of the

fluorescence is a little bit more than zero (dip on the right-hand side of Fig. 6 b), the transition rate of trapped lithium atoms to the highly-excited state is of the order of the MOT loading rate $1/\tau_{\text{dec}} \sim 0.1 \text{ s}^{-1}$ (see Fig. 5). By taking into account the transition rate and relaxation processes, the evaluated number of atoms in the Rydberg state is much less than the number of atoms in the ground states. In Fig. 7, the dips corresponding to the states $114S_{1/2}$, $114D_{3/2}$, and $114D_{5/2}$ are shown. The components of the $114D$ -state are not completely resolved due to a large spectral broadening. The measured average frequencies of transitions $2P_{3/2} - 114S_{1/2}$ and $2P_{3/2} - 114D_{3/2}$ are $856647.1(3)$ and $856648.6(3)$ GHz, respectively.

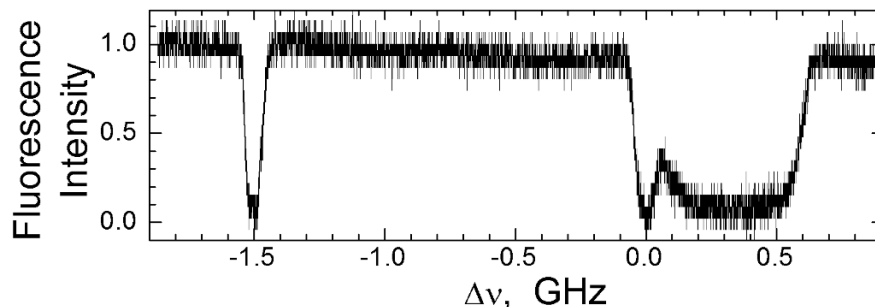


Fig. 7. Resonance fluorescence of the trapped atoms on transitions $2P_{3/2} - 114S$ and $2P_{3/2} - 114D$ recorded with slow scan of the laser frequency.

The isolated resonance (the dip), which corresponds to the transition $2P_{3/2} - 114S$, shows a minimum spectral width of 0.1 GHz. The S-states ($l = 0$) are less sensitive to external perturbations in comparison with the D-states ($l = 2$). We would like to reduce the width of the resonances by changing powers of the laser beams, magnetic field gradient, and other experimental parameters. Probably, the stray electric field in the vacuum camera should be suppressed. Also interactions between Rydberg atoms may contribute to the spectral width of the resonances.

We plan to study Rydberg atoms by recording the emitted light at the transition $3P - 2S$ (323 nm) induced by applying the laser field at selected $n\ell - 3P$ transitions (797 nm). It will be great to detect the appearance of long-range interactions between Rydberg atoms [19,20].

5. Summary

To summarize, we list the main results of this study.

We demonstrated the cw two-step excitation of Rydberg lithium atoms in the magneto-optical trap. Lithium atoms were excited using the ultraviolet laser system. For identification of the Rydberg transitions, we recorded the resonance fluorescence of ultracold lithium atoms. In our work, the first results on high-resolution spectroscopy of several S and D Rydberg states of ${}^7\text{Li}$ atoms ($n > 40$) are presented and discussed.

Acknowledgments

We thank M. A. Gubin, V. V. Vasilliev, V. L. Velichansky, and S. A. Zibrov (Lebedev Physical Institute, Moscow), V. N. Kulyasov (Vavilov State Optical Institute, St. Petersburg), I. I. Ryabtsev

(Rzhanov Institute of Semiconductor Physics, Novosibirsk), A. V. Turlanov (Institute of Applied Physics, Nizhni Novgorod), N. B. Buyanov (Newport Corporation, USA), A. M. Akul'shin and A. I. Sidorov (Swinbourne University of Technology, Melbourne, Australia), and M. N. Shneider (Princeton University, USA) for valuable discussions, critical remarks, and helpful assistance. This work was supported by the Russian Science Foundation under Project No. 14-12-01279.

References

1. T. F. Gallagher, *Rydberg Atoms*, Cambridge University Press, Cambridge (2005).
2. V. Fortov, I. Iakubov, and A. Khrapak, *Physics of Strongly Coupled Plasma*, Oxford University Press, Oxford (2006).
3. E. A. Manykin, M. I. Ozhovan, and P. P. Poluektov, *Sov. Phys. Dokl.*, **26**, 974 (1981).
4. E. A. Manykin, M. I. Ozhovan, and P. P. Poluektov, *Sov. Phys. JETP*, **75**, 440 (1992).
5. T. Pohl, E. Demler, and M. D. Lukin, *Phys. Rev. Lett.*, **104**, 043002 (2010).
6. P. Schaus, M. Cheneau, M. Endres, et al., *Nature*, **491**, 87 (2012).
7. J. Deiglmayr, M. Reetz-Lamour, T. Amthor, et al., *Opt. Commun.*, **264**, 293(2006).
8. B. A. Bushaw, W. Nörtershäuser, G. W. F. Drake, and H.-J. Kluge, *Phys. Rev. A*, **75**, 052503 (2007).
9. A. K. Mohapatra, T. R. Jackson, and C. S. Adams, *Phys. Rev. Lett.*, **98**, 113003 (2007).
10. E. Brekke, J. O. Day, and T. G. Walker, *Phys. Rev. A*, **78**, 063830 (2008).
11. U. Schunemann, H. Engler, M. Zielonkowski, et al., *Opt. Commun.*, **158**, 263 (1998).
12. K. Martyanov, V. Makhalov, and A. Turlapov, *Phys. Rev. Lett.*, **105**, 030404 (2010).
13. B. B. Zelener, S. A. Saakyan, V. A. Sautenkov, et al., *JETP Lett.*, **98**, 670 (2014).
14. B. B. Zelener, S. A. Saakyan, V. A. Sautenkov, et al., *J. Exp. Theor. Phys.*, **119**, 795 (2014).
15. V. Vuletic, V. A. Sautenkov, C. Zimmermann, and T. W. Hansch, *Opt. Commun.*, **108**, 77 (1994).
16. I. I. Sobelman, *Atomic Spectra and Radiative Transitions*, Springer, Berlin (1979).
17. B. B. Zelener, S. A. Saakyan, V. A. Sautenkov, et al., *JETP Lett.*, **100**, 366 (2014).
18. S. Bubin and L. Adamowicz, *Phys. Rev. A*, **87**, 042510 (2013).
19. I. I. Ryabtsev, I. I. Beterov, D. B. Tretyakov, and V. M. Entin, *Phys. Rev. Lett.*, **104**, 073003 (2010).
20. T. Pohl, C. S. Adams, and H. R. Sadepour, *J. Phys. B: At. Mol. Opt. Phys.*, **44**, 180201 (2011).